Experimental Study of Prestressed Composite Beams

By Hamid Saadatmanesh,[1] Associate Member, ASCE, Pedro Albrecht,[2] Member, ASCE, and Bilal M. Ayyub,[3] Member, ASCE

Abstract: The concept of prestressing steel structures has only recently been widely considered, despite a long and successful history of prestressing concrete members. Several analytical studies of prestressed composite beams were reported in the literature, but much of that work was not experimentally verified. In particular, no test results were found on prestressed composite beams subjected to negative bending moment. This paper examines experimentally the behavior of prestressed, composite steel-concrete beams. Two beams were tested, one subjected to positive bending moment and the other to negative bending moment. The load was plotted against the deflection, and the strains in the concrete, steel beam, and prestressing bars. The values predicted with the equations of internal force equilibrium and compatibility between the deformations of the bars and the composite beam were found to correlate well with the measured data.

Introduction

Composite steel-concrete beams prestressed with high-strength steel bars or cables offer four major advantages: (1) Elastic behavior to higher loads; (2) increased ultimate capacity; (3) reduced structural steel weight; and (4) improved fatigue and fracture behavior (Saadatmanesh et al. 1986).

Both simple and continuous beams can be prestressed. In the positive moment region, the steel beam is prestressed along the bottom (tension) flange before the concrete deck is cast because the negative moment induced by prestressing could otherwise cause the concrete to crack in tension. In the negative moment region, the steel beam and the concrete deck can be prestressed either separately or jointly along the top (tension) flange. This places the concrete in compression, prevents cracking under service loads, and increases the stiffness of the girder.

Prestressed composite beams can be used in new construction as well as in upgrading existing structures. As an example of the latter case, the moment carrying capacity of the girders can be increased by prestressing the steel girders when the deck of an existing bridge is being replaced.

Applications

Prestressed steel members have been used for some time in building and bridge construction. Some illustrative examples documented in the literature are cited below.

A 152 m (500 ft) long, two-span, continuous, prestressed steel truss supports the roof of a hangar at the Melsbrock Airport in Brussels, Belgium (Magnel 1954). The tension chords of the truss were prestressed with four cables, each consisting of 64 wires of 7 mm (0.276 in.) diameter, after the steel structure had been erected. Prestressing reduced the weight of the truss by 12% and the cost by 4%. Generally, the longer the span the greater was the savings. In the case of the hangar, increasing the total length of the truss to 183 m (600 ft), would have reduced the weight by 25% and the cost by 18%.

The Liverly Street Bridge in Birmingham, England carries a busy highway over mainline railroad tracks (Berridge and Donovan 1956). To make up for the severe corrosion induced by the smoke from coal-fired locomotives, the weakened tension chord of each truss was prestressed with a force of 2,220 kN (500 kip) applied through eight high-strength bars of 25 mm (1 in.) diameter and 1,070 MPa (155 ksi) tensile strength. Four bars were placed on each side of the chord and anchored to large welded steel brackets. Prestressing not only restored the loss in strength due to corrosion, but it also increased the load carrying capacity by 12% above that of the original structure.

In South Africa, near the town of Brits, a 101 m (330 ft) long four-span bridge was designed to carry very heavy truck loads (Anon 1964). Two lightweight, thin-walled steel box girders, spaced 6.1 m (20 ft) on centers, support the 11 m (36 ft) wide concrete deck without cross bracing. Each girder was prestressed with a force of 3,200 kN (720 kip) applied with nine cables, each having 12 strands of 7 mm (0.276 in) diameter wire. The wires were placed inside the girder next to the tension flange and were anchored at the girder ends. Major advantages claimed for the new design included savings in weight and material cost, ease of erection of the completely shop fabricated girders, and speed of construction. The designers also reported that, for comparable spans and loadings, five or six nonprestressed steel or prestressed concrete girders would be needed to carry the same load.

Prestressed steel trusses support three new parking levels above the existing Port Authority Bus Terminal in New York (Cetra 1961). The Warren trusses are 61 m (200 ft) long, spaced 15.2 m (50 ft) apart, and were prestressed with high-strength steel cables along the bottom chord. The height of the truss was a very critical parameter in this structure, and prestressing made shallower depths possible. Furthermore, prestressing reduced the cost as compared to a nonprestressed structure.

In California, three span continuous, prestressed, composite steel girders support a three-story apartment building constructed above the basement parking areas (Anon 1964). The positive moment region in the center span of each girder was prestressed with high-strength steel wires placed above the tension flange. The prestressing force in each girder was 890 kN (200 kip). Because prestressing the positive moment regions of a continuous girder induces positive moments over the interior supports, the tensile stress in the concrete and the compressive stress in the bottom flange of the steel beam at the interior supports were reduced from 4.4–2.5 MPa (640–360 psi), and 167–119 MPa (24.2–17.2 ksi), respectively. Prestressing also reduced the tensile stress in the bottom flange at the center span from 190–119 MPa (27.5–17.2 ksi).

The recent design of the Bonners Ferry Bridge in Northern Idaho effectively utilizes the prestressed girder concept (Seim et al. 1982). The four-

[1]Asst. Prof., Dept. of Civ. Engrg. and Engrg. Mech., Univ. of Arizona, Tucson, AZ 85721.
[2]Prof., Dept. of Civ. Engrg., Univ. of Maryland, College Park, MD 20742.
[3]Assoc. Prof., Dept. of Civ. Engrg., Univ. of Maryland, College Park, MD.

Note. Discussion open until February 1, 1990. Separate discussions should be submitted for the individual papers in this symposium. To extend the closing date one month, a written request must be filed with the ASCE Manager of Journals. The manuscript for this paper was submitted for review and possible publication on June 26, 1987. This paper is part of the *Journal of Structural Engineering*, Vol. 115, No. 9, September, 1989. ©ASCE, ISSN 0733-9445/89/0009-2348/$1.00 + $.15 per page. Paper No. 23389.

lane, four-girder steel bridge was bid below the concrete alternate. The spans of the 420 m (1,378 ft) long, continuous-span bridge vary from 30.5–47.2 m (100–155 ft). The negative moment regions were prestressed in two stages. First, the steel girders were prestressed along the top flange before the concrete deck was cast. Second, the concrete deck was posttensioned longitudinally to oppose the tensile stresses induced by the applied load, and transversely to permit wider girder spacing. Since the prestressing of this bridge keeps the deck always in compression over the negative moment regions, the girders are composite over the entire length. The positive moment regions were not prestressed.

After the new California permit loads were introduced, many bridges in that state had to be upgraded (Mancarti 1984). The Pit River Bridge on Interstate Highway I-5 in Shasta County was strengthened by adding prestressing bars in the negative moment regions. The six simple-span, five-girder, composite bridge on California highway CA-99 over Avenue 328 was found to be deficient in moment-carrying capacity for new permit loading in the three central, 27.4 m (90 ft) long spans. The bridge was strengthened by adding two tendons to each deficient girder. The tendons were placed 150 mm (6 in.) above the bottom (tension) flange and prestressed to 267 kN (60 kip) per tendon. Also strengthened were the Truckee River Bridge on I-80, Route 43 and I-5 separation on CA-43, and three bridges on CA-101 between Santa Barbara and Monterey.

Other examples of prestressing steel structures are cited in the literature. It appears that most were built in Europe.

Previous Experimental Work

The authors have found in the literature the results of five experimental studies on the behavior of prestressed composite beams.

Tachibana et al. (1964) tested three prestressed, composite model bridges. Bridge A was simply supported and Bridges B and C were two-span-continuous. The simple-span Bridge A was 4 m (13 ft) long and had a 60 mm (2.4 in.) thick by 1,200 mm (47.2 in.) wide concrete deck compositely connected to two steel beams spaced 600 mm (23.6 in.) apart. The individual spans of the two continuous-span Bridges B and C were similar to that of Bridge A. All beams had 90 × 8 mm (3.5 × 5/16 in.) flanges and a 350 × 8 mm (13.8 × 5/16 in.) web. The beams, whether of simple or continuous span, were prestressed full length with 24 mm (15/16 in.) diameter high-strength steel bars running along the bottom flange in the positive moment region. The bars were draped at all interior and exterior supports. The steel beams in Bridges A and C were prestressed before the concrete deck was cast, and in Bridge B after the concrete deck was cast. The calculated elastic deflections and changes in the tendon force were comparable to the measured values. The inelastic behavior was not predicted. The concrete deck over the interior support of Bridge C cracked at a smaller load than in Bridge B, leading the researchers to conclude that a negative moment region should be prestressed after the concrete deck is cast.

Stras (1964) tested three simple-span, prestressed, composite beams subjected to positive bending moment. The W 8 × 10 steel beams were prestressed with a 10 mm (3/8 in.) diameter high-strength steel cable running 22 mm (7/8 in.) below the tension flange along the full beam length and

then compositely connected to a cast-in-place 455 mm (18 in.) wide by 76 mm (3 in.) thick concrete slab. The measured strains in the concrete slab, steel beam, and cable compared reasonably well with the calculated values.

Murkowski (1974) tested a prestressed truss that had one top chord and two bottom chords of tubular cross-section in a triangular arrangement, with radial struts maintaining the distance between the three chords. The truss had no diagonals. This type of member may be suited for supporting light roofs of industrial buildings. Prestressing increased the elastic load carrying capacity and the buckling strength of the top chord. The results obtained from a model test confirmed the calculation of the change in the prestressing force due to the applied loads. Additional investigations needed to implement this type of truss in engineering practice were outlined.

Ferjencik and Tochacek (1980) tested six simple-span, rolled beams prestressed with straight, high-strength, steel wires placed below the tension flange. The magnitude of the prestressing force was chosen so as to prevent yielding of the bottom flange. As in previous studies, the measured elastic strains through the beam depth compared well with the predicted strains, except that the measured change in tendon force was smaller than calculated.

Klaiber et al. (1983) tested four 7.9 m (26 ft) long prestressed, composite steel girders that were sawed from a half-scale model of an existing simple-span bridge, which did not have enough moment carrying capacity nor shear connectors for current permit loads. Shear connectors were added to two of four beams. Each composite beam was posttensioned with two 16 mm (5/8 in.) diameter high-strength steel bars located 57 mm (2-1/4 in.) above the tension flange. The test variables were the addition of shear connectors and the level of prestressing, neither of which was found to significantly affect the elastic load-displacement behavior of the beams. The two beams with added shear connectors exhibited less slip and eventually failed by crushing of the concrete. The third beam failed at the shear connectors. The test of the fourth beam was discontinued prior to reaching the ultimate load. The increase in the posttensioning force with applied load was neglected in the theoretical analysis.

Positive Moment Region Test

Two beams were tested in the present study. Beam A had prestressing bars along the bottom (tension) flange and was subjected to positive bending moment. Beam B had bars along the top (tension) flange and was subjected to negative bending moment.

Specimen

The 4.57 m (15 ft) long Beam A, shown in Fig. 1, had a 915 mm (3 ft) wide by 76 mm (3 in.) thick concrete slab compositely connected to a W 360 × 45 (W 14 × 30) rolled beam of ASTM A588 steel. Pairs of 13-mm (1/2 in.) diameter by 51 mm (2 in.) long shear studs were welded to the top flange, 120 mm (4-3/4 in.) on centers, between the load points and the supports. The temperature and shrinkage reinforcement consisted of 10 mm (3/8 in.) diameter deformed bars, three spaced longitudinally at 229 mm (9 in.) on centers and 11 transversely at 455 mm (18 in.) on centers. Four pairs of 76 × 13 × 330 mm (3 × 1/2 × 13 in.) long bearing stiffeners were

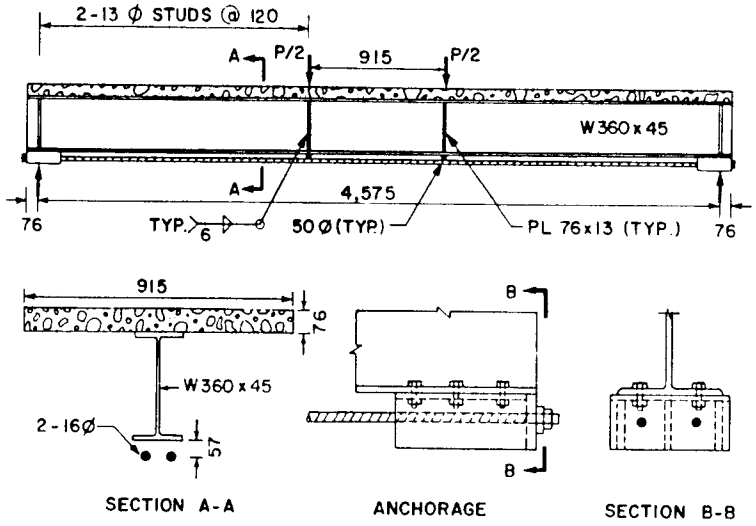

FIG. 1. Beam A Subjected to Positive Moment

welded to the steel beam at the supports and loading points.

The steel beam was prestressed with two 16 mm (5/8 in.) diameter Grade 150 DYWIDAG Threadbars (DYWIDAG Systems International 1984) running the full beam length 57 mm (2-1/4 in.) below the bottom (tension) flange (Fig. 2). They were anchored at the ends with a welded, open box consisting of a flange, three webs and an end plate as shown in Fig. 3. The box was bolted to the bottom flange of the beam. Each bar was stressed to 50 percent of its tensile strength, that is, 98 kN (22 kip). The steel beam

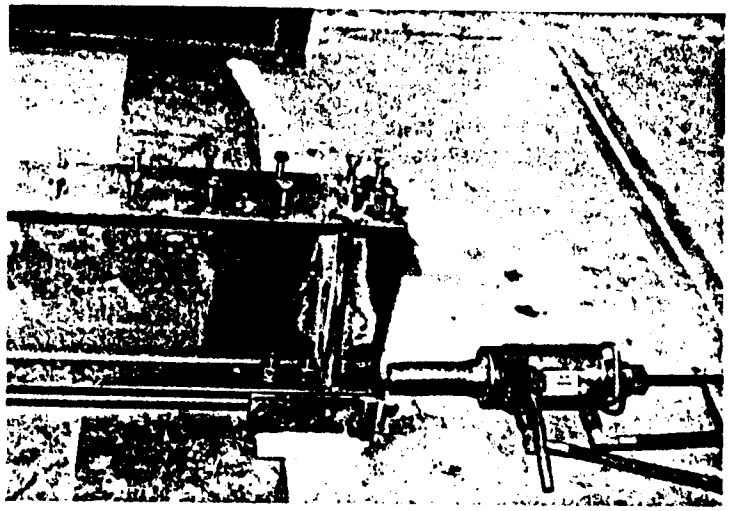

FIG. 2. Prestressing of Beam A

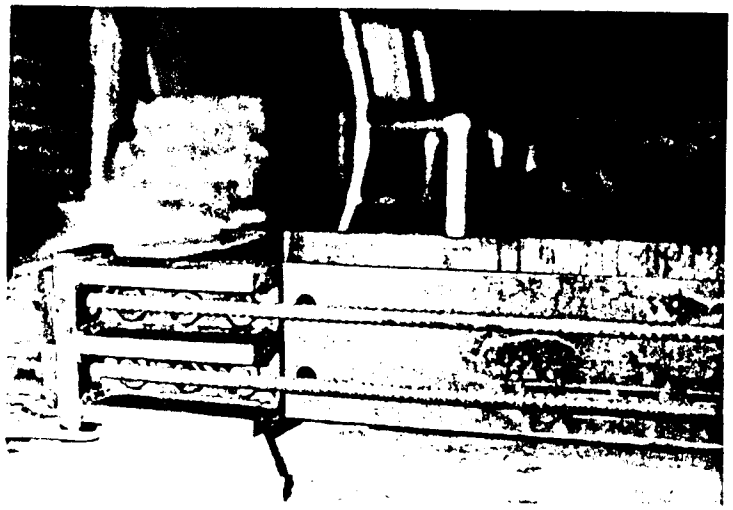

FIG. 3. Anchorage of Bars in Beam A

was prestressed before the concrete slab was cast to prevent the concrete from cracking under tension.

Placing the bars below the tension flange increased the lever arm and maximized the benefit of the bar forces. For grade separation structures with limited clearance the bars may have to be located above the tension flange for protection against collision by overheight trucks.

MATERIALS

Concrete

The concrete mix for the slab was designed to give a compressive strength of 27.6 MPa (4.0 ksi). The measured compressive strength of the three cylinders, cast from the same concrete and cured for the same 90-day length of time as the slab, was 33.4 MPa (4.85 ksi). The tensile strength measured with three split-cylinder tests was 3.0 MPa (0.44 ksi).

Steel Beam

The steel used for the W 14 × 30 beams conformed to the tensile and chemical requirements of ASTM A588 Standard Specification for High-Strength, Low-Alloy Steel with 345 MPa (50 ksi) Minimum Yield Point to 100 mm (4 in.) thick. The mean tensile properties of three test specimens cut from the web of the beam were 367 MPa (53.3 ksi) yield stress, 520 MPa (75.4 ksi) tensile strength, and 24% elongation.

Prestressing Bars

The tensile properties of the bars, measured with three full-diameter specimens, were 910 MPa (132 ksi) yield stress, 1,090 MPa (158 ksi) tensile strength, and 9.7% elongation. Fig. 4 shows typical, measured stress-strain curves. The bars exhibited a yield plateau prior to strain hardening. They were less ductile than the steel beam.

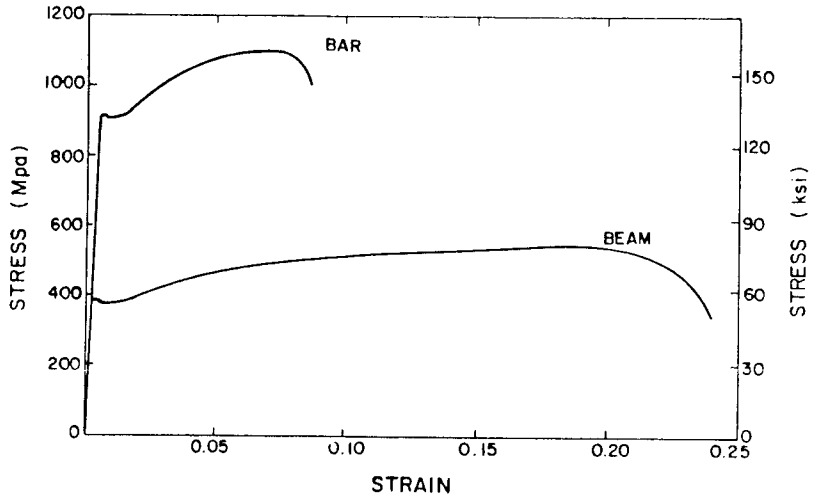

FIG. 4. Measured Stress-Strain Curves of Beam and Bar

The manufacturer supplied data on stress relaxation of the bars as a function of prestressing level and time. According to these data, the stress in the bars relaxed by one percent between the time of prestressing and the time when the beam was tested.

Instrumentation

Fig. 5 shows the instrumentation of beam A at midspan. Before the beam was prestressed, five strain gages were mounted on each flange, and two pairs of diametrically opposed strain gages were installed on each bar. After the concrete had hardened, five EP-08-20CBW-120 strain gages were mounted

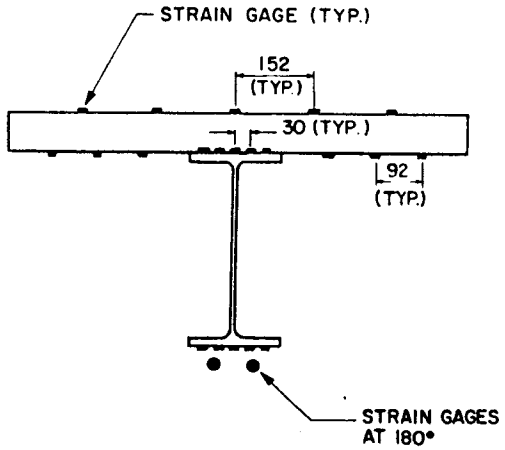

FIG. 5. Strain Gages Mounted at Midspan of Beam A

on the top surface and six on the bottom surface of the slab. The mid-span deflection was measured with two displacement gages located above the tension flange on either side of the web.

Beam A was loaded in increments of load in the elastic region and in increments of displacement in the inelastic region. The strain and displacement gages were read after a 15-minute waiting period at each increment. The test machine was screw driven, providing displacement-controlled loading.

Results

Measured Load-Deflection Curve

The measured load-deflection behavior is shown in Fig. 6 with solid lines. The behavior was initially linear elastic. At a load of 356 kN (80 kip), the bond broke between the top flange and the concrete slab, causing the slab to slip into full bearing against the shear studs and the load to drop to 329 kN (74 kip). The extreme fiber of the tension flange yielded at a measured load of about 445 kN (100 kip). Thereafter, the stiffness of the beam gradually decreased, and the load-deflection curve became progressively nonlinear as the yielding extended through the flange and into the web. At a load of 512 kN (115 kip) the bars yielded, thus making the load-deflection curve more nonlinear. At 578 kN (130 kip), the beam was completely unloaded and then reloaded. The unload-reload loop exhibited a slight hysteresis, but the loop closed at the same point at which the beam had been unloaded. At 641 kN (144 kip), the beam failed by crushing of the concrete slab in compression. The compression flange of the steel beam was supported by the compositely connected slab and did not buckle either locally or laterally. The bearing stiffeners prevented web crippling. No transverse cracks were observed in the slab.

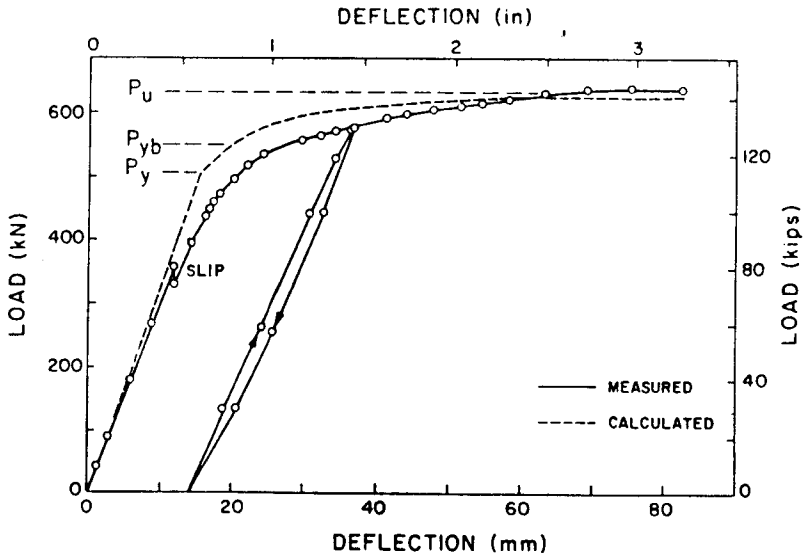

FIG. 6. Load-Deflection Curve of Beam A

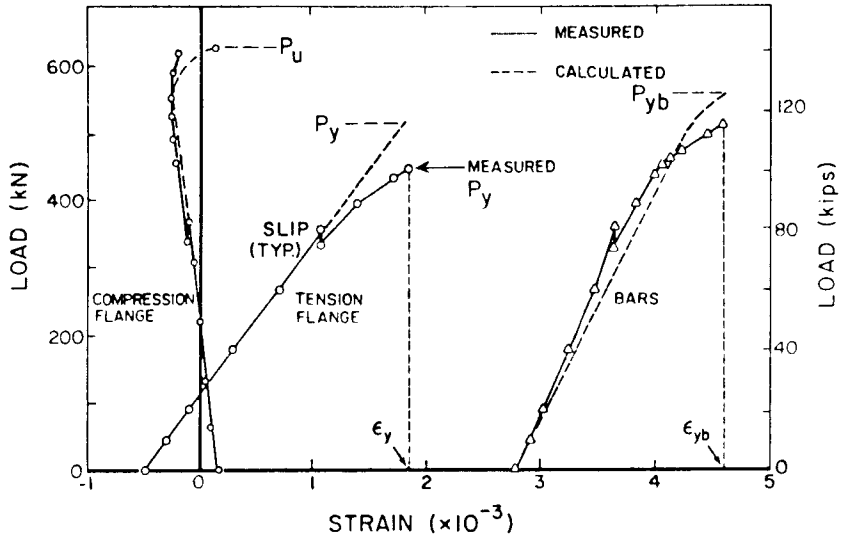

FIG. 7. Load-Strain Curves for Bars and Flanges of Beam A

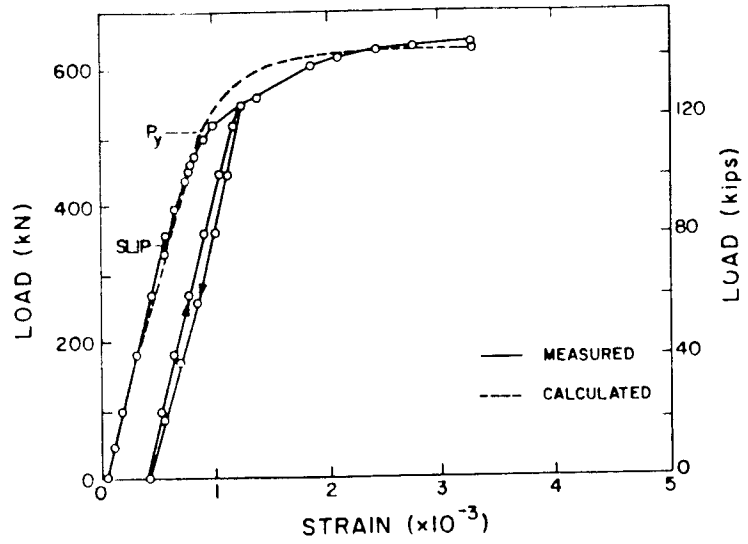

FIG. 8. Load-Strain Curve for Extreme Concrete Fiber of Beam A

The shear studs were designed for a concrete strength of 27.6 MPa (4,000 psi), while the measured strength of the concrete was 33.4 MPa (4,850 psi). As a result, relative to the higher concrete strength, the shear studs were underdesigned by 21%. This incomplete composite action induced somewhat higher shear stud deformations than would have otherwise occurred.

Calculated Load-Deflection Curve

The deflections, stresses, and strains in the elastic and inelastic regions were calculated with an incremental deformation method, ensuring compatibility of deformations and equilibrium of forces, and using the measured compressive strength of the concrete and yield strength of steel and bars (Saadatmanesh et al. 1986). The calculated load-deflection behavior of Beam A is shown with dashed lines in Fig. 6. Also shown are the calculated load levels at which the tension flange of the steel beam yielded, P_y = 512 kN (115 kip), the bars yielded, P_{yb} = 552 kN (125 kip), and the ultimate strength was reached, P_u = 641 kN (144 kip).

In the elastic region, up to the slip load, the measured and calculated load-deflection curves correlated well. Following slip, the calculated deflection was smaller than the measured deflection because the analysis assumed rigid shear stud behavior whereas the beam exhibited incomplete composite action and shear stud deformation. The measured ultimate load correlated well with the calculated limit load.

Measured Load-Strain Curves

The solid lines in Fig. 7 show the measured curves of load versus strain in the bars and the two flanges of the steel beam. The strains in the bars and tension flange were recorded up to yielding of the respective steels. The compression flange remained elastic throughout the test. All curves were offset from the origin of the coordinate system by the initial prestressing strains. The dead load strains were negligible. All load-strain curves were linear up to slip. Thereafter, the curves became progressively nonlinear with increasing load.

The measured strains in the compression flange began to level out at 520 kN (117 kip) load and thereafter decreased because the neutral axis shifted upward after first the tension flange yielded and then the bars. In the elastic region, the neutral axis was located in the web of the steel beam, 310 mm (12.2 in.) from the bottom of the tension flange. At the ultimate load, the calculated neutral axis was located 2.5 mm (0.1 in.) into the concrete whereas the measured neutral axis was below the extreme fiber of the compression flange. This difference was caused by the incomplete composite action.

The intersections of the vertical lines, drawn at the measured yield strains ϵ_y and ϵ_{yb} (Fig. 7), with the load-strain curves indicate the loads at which the tension flange and the bars yielded. By comparing the load-strain curves of the tension flange and the bars, it can be seen that the strain in the bars rapidly increased after the tension flange reached its yield strain, suggesting that the bars began to carry a proportionally greater fraction of the tensile component of the internal moment couple.

Calculated Load-Strain Curves

The calculated load-strain curves for the flanges and the bars are shown with dashed lines in Fig. 7. Also shown are the calculated loads at which the tension flange of the steel beam yielded, P_y, the bars yielded, P_{yb}, and the concrete crushed, P_u. Like the load-deflection curve of Fig. 6, the measured and calculated load-strain curves correlated well up to slip load. Following slip, the measured strains were larger than calculated due to incomplete composite action and deformation of the shear studs.

The measured load-strain curve for the extreme fiber of the concrete slab, shown in Fig. 8, was initially linear. As was observed for the tension flange,

the load dropped at slip but the linear behavior continued with increasing load until the extreme fiber of the tension flange yielded. The unload-reload segment exhibited a closed hysteresis loop. With progressive yielding of the steel beam and the bars, the load-strain curve of the concrete became nonlinear until the concrete eventually crushed at a strain of 0.0034 mm/mm. The calculated load-strain curve of the concrete, shown dashed in Fig. 8, correlated well with the measured behavior in the elastic region and at the ultimate load.

Negative Moment Region Test

Specimen

Beam B simulated the negative moment region of a continuous beam between the inflection points on each side of an interior support. However, two symmetrical reaction points spaced 915 mm (36 in.) apart were provided to create a region of constant, negative moment for better observation of the moment-rotation behavior (Fig. 9).

The 4.57 m (15 ft) long Beam B, shown in Fig. 9, had a 455 mm (18 in.) wide by 76 mm (3 in.) thick concrete slab compositely connected to a W 360 × 45 (W 14 × 30) rolled A588 steel beam. Pairs of 13-mm (1/2 in.) diameter by 51 mm (2 in.) long shear studs were placed at 610 mm (24 in.) on centers between each load point and the nearby support. The temperature and shrinkage steel consisted of two 10-mm (3/8 in.) diameter deformed bars placed longitudinally at 152 mm (6 in.) on centers and ten transversely at 455 mm (18 in.) on centers. Four pairs of 76 × 16 × 330 mm long (3 × 5/8 × 13 in.) bearing stiffeners were welded to the beam at the supports and loading points.

The composite beam was prestressed, after the concrete slab had been cast, with two 16-mm (5/8 in.) diameter Grade 150 DYWIDAG Threadbars located 24 mm (15/16 in.) below the top (tension) flange, running the full

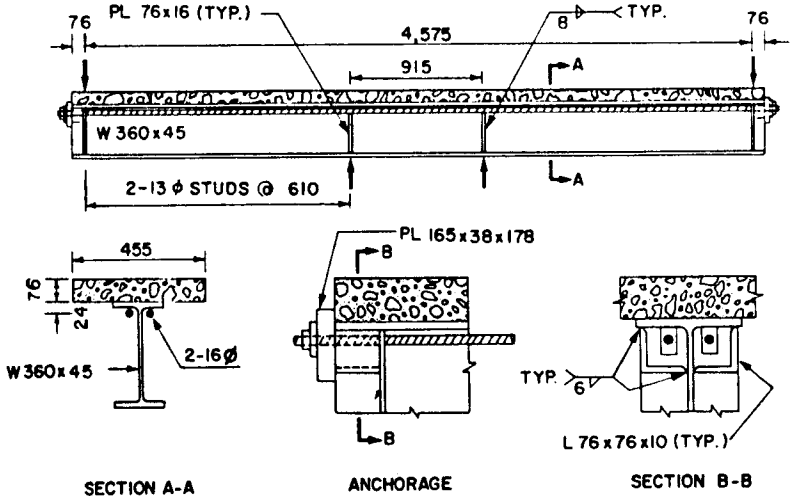

FIG. 9. Negative Moment Test (Beam B)

length of the beam. Because the bars were 56 mm (2.2 in.) above the centroidal axis of the composite section, prestressing placed the concrete slab under compression. Hence, the entire composite section could be prestressed without cracking the concrete. The end anchorages of the bars consisted of two angles welded to the steel beam and an end plate, as shown in Fig. 9.

Materials

The mechanical properties of the concrete and steel for Beam B were measured following the procedures previously described for Beam A. The concrete had a compressive strength of 32.4 MPa (4.70 ksi) and a tensile strength of 2.8 MPa (0.41 ksi). The concrete cylinders were cast from the same concrete and cured for the same 60 day length of time as the slab of Beam B. The steel beam had 379 MPa (55.0 ksi) yield strength and 530 MPa (76.9 ksi) tensile strength, and 26 percent elongation.

Instrumentation

The strain gages were mounted at midspan of Beam B in a manner similar to that shown in Fig. 5 for Beam A.

The loads were applied on Beam B with a manually operated hydraulic jack (Fig. 10). For convenience of loading, Beam B was tested upside down, with the hydraulic jack acting as an interior support of a continuous beam and the reactions at the ends of Beam B acting as the shear at the inflection points. The beam was tested in load increments in the elastic region and in displacement increments in the inelastic region.

Results

Measured Load-Deflection Curve

The measured load-deflection curve, shown solidly in Fig. 11, exhibited a bilinear behavior in the elastic region caused by the change in stiffness as

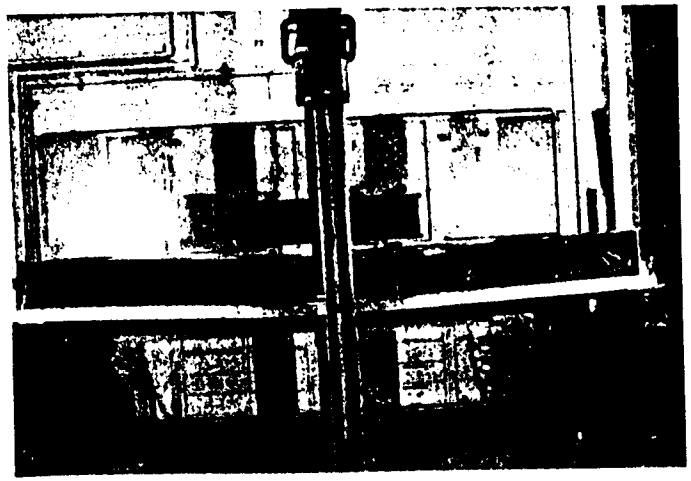

FIG. 10. Test Setup for Beam B

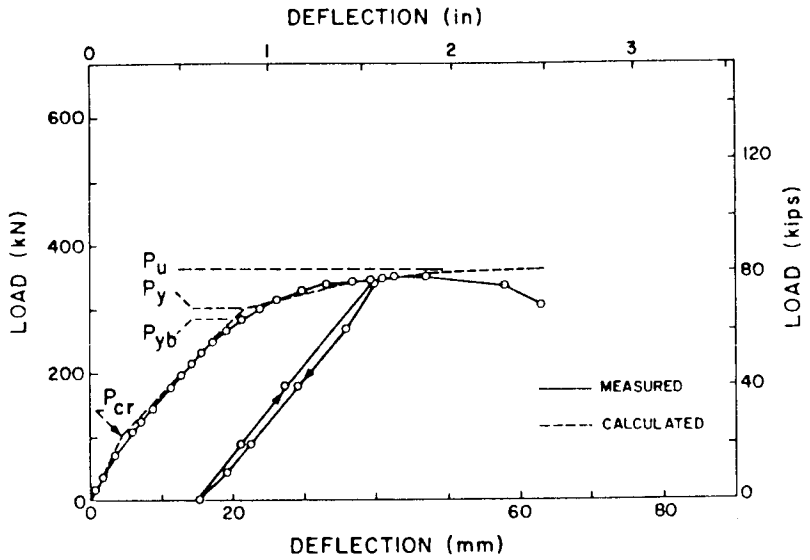

FIG. 11. Load-Deflection Curve of Beam B

the concrete slab cracked at a tensile stress of 1.7 MPa (244 psi) induced by a 71 kN (16 kip) load. At 289 kN (65 kip), the extreme fiber of the compression flange of the steel beam yielded, resulting in a progressively nonlinear load-deflection curve as yielding extended into the web. At 338 kN (76 kip), the bars yielded, the beam stiffness further decreased, and the load-deflection curve flattened. At 347 kN (78 kip), the ultimate load was reached as the compression flange began to buckle locally.

Calculated Load-Deflection Curve

The calculated load-deflection curve is shown with dashed lines in Fig. 11. Also shown are the calculated loads at which the concrete slab cracked, P_{cr}, the bars yielded, P_{yb}, the compression flange of the steel beam yielded, P_y, and the beam reached its ultimate load, P_u. The measured load-deflection curve correlated very well with the calculated curve up to the ultimate load. The difference between the two curves beyond the ultimate load was due to local buckling of the compression flange, which was not modeled in the calculations.

Measured Load-Strain Curves

The measured curves of load versus strain in the bars and in the two flanges of the steel beam are shown with solid lines in Fig. 12. The load-strain curves are offset from the origin of the coordinate system by the strains induced during the initial prestressing. The tension flange and the bars exhibited an elastic bilinear behavior due to the change in stiffness when the concrete slab cracked and the force in the deck was transferred to the tension flange and the bars.

The intersection of the vertical lines at the measured yield strains, ϵ_y and

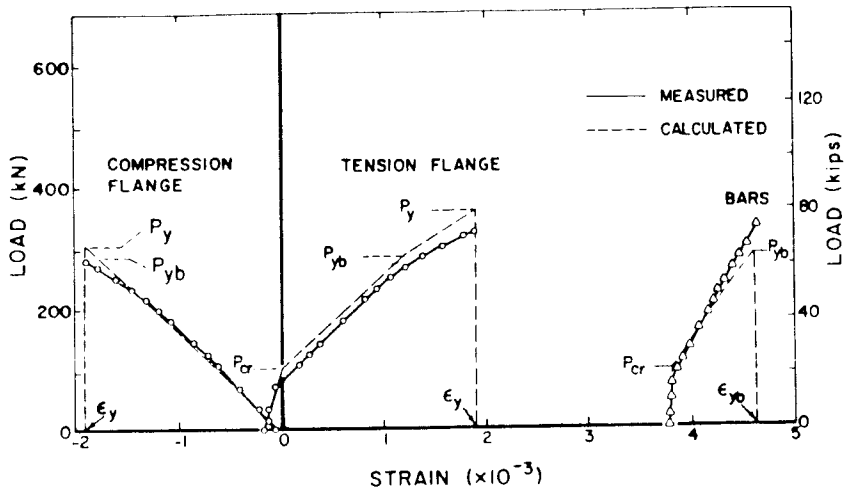

FIG. 12. Load-Strain Curves for Bars and Flanges of Beam B

ϵ_{yb}, with the load strain curves indicate the loads at which the two flanges and the bars yielded.

Calculated Load-Strain Curves

The calculated curves of load versus strain in the bars and in the two flanges of the steel beam are shown with dashed lines in Fig. 12. In the region of elastic behavior, the calculated strains in the bars and compression flange correlated very well with the measured strains. The small difference between the calculated and measured strains in the tension flange above P_{cr} was caused by cracking of the concrete slab at a load lower than predicted with the measured split tensile strength. As a result, the concrete's tensile component of the internal moment was shifted to the tension flange at a lower load. The nearly parallel lines of calculated and measured elastic strains in the tension flange above P_{cr} confirmed that the difference between the two was caused by the onset of early cracking. The model correctly predicted the stiffness of the cracked composite beam.

Conclusions

The following conclusions can be drawn from the test results:

1. Adding prestressed bars to composite beams significantly increased the yield load and the ultimate load.
2. The farther the bars are located from the neutral axis, the greater is the increase in strength. For this reason, the bars should be located below the bottom (tension) flange in the positive moment region and above the top (tension) flange in the negative moment region. When the bars must be protected against impact damage from overheight trucks in grade separation structures, the bars may have to be placed above the bottom (tension) flange in the positive moment region.
3. An adequate number of guides are needed to ensure that the bars follow

the beam curvature. In this way the deflection of the beam does not reduce the eccentricity of the bar and, hence, the ultimate moment carrying capacity of the beam.

4. Sufficient prestressing of the negative moment region can prevent the concrete from cracking under service loads. This increases the stiffness and reduces the deflection. The absence of flexural cracks may extend the service life of the deck.

5. The beneficial effects of prestressing the composite beam in the negative moment region can be achieved with less prestressing force, if the steel beam and the deck are separately prestressed and then compositely connected. In this case, the shear studs should be welded to the flange in clusters, and the openings provided in the deck for the shear studs should be grouted after the beam and the deck are prestressed.

6. Adding bars to either the positive or negative moment regions reduces the stress in the concrete deck because the increase in bar force with applied load produces a counteracting moment.

7. Equations of equilibrium of internal forces and compatibility of deformations predicted very well the stresses and strains throughout the full range of loading up to failure.

The writers are performing additional work on the behavior of prestressed, composite steel-concrete beams. Models for predicting the elastic and inelastic behavior of prestressed, composite beams are described in the companion paper (Saadatmanesh et al. 1989). Tests currently underway at the University of Maryland are examining the fatigue behavior of prestressed, composite beams.

Acknowledgment

The writers are grateful to Dr. Charles Culver, who made the facilities at the National Bureau of Standards available for testing the beams.

Appendix. References

Berridge, P. S. A., and Donovan, L. H. (1956). "Prestressing restores weakened truss bridge." *Civil Engineering*, 26(9), 48–49.
Cetra, M. A. (1961). "Bus terminal extended upward three stores." *Civil Engineering*, Oct. 1961.
"DYWIDAG threadbar post-tensioning system." (1984). *Brochure No. 2M DSI #4C*, DYWIDAG Systems International, Lincoln Park, N.J.
Ferjencik, P., and Tochacek, K. M. (1980). "Economical design of prestressed plate girders." Slovak School of Higher Technology, Czechoslovakia, Stavebnicky Cas, 28(4), 273–287.
Klaiber, F. W., et al. (1983). "Strengthening of existing single span steel beam and concrete deck bridges." Engineering Research Institute, Dept. of Civ. Engrg., Iowa State University, Ames, Iowa.
Magnel, G. P. (1954). "Long prestressed steel truss erected for Belgian hangar," *Civil Engineering*, 24(10), 38–39.
Mancarti, G. D. (1984). "Strengthening California steel bridges by prestressing." *Transportation Research Record 950*, Second Bridge Engineering Conf., Transportation Research Board, 183–187.
Murkowski, W. (1974). "Experimental testing of new type of prestressed steel girder." Poznan Polytechnic, Poland, Archives of Civil Engineering, 20(4), 699–712.

"Prestressed steel makes a bridge." Eng. News Rec., November 5, 1964.
"Prestressed steel girders carry prestressed concrete floor." Eng. News Rec., Mar. 26, 1964.
Saadatmanesh, H., Albrecht, P., and Ayyub, B. M. (1986). "Static strength of prestressed composite steel girders." *Civil Engineering Report*, Univ. of Maryland, College Park, Md.
Saadatmanesh, H., Albrecht, P., and Ayyub, B. M. (1989). "Analytical study of prestressed composite beams." *J. Struct. Engrg.*, ASCE, 115(9), 2365–2382.
Saadatmanesh, H., Albrecht, P., and Ayyub, B. M. (1989). "Design guidelines for prestressed composite beams," *J. Struct. Engrg.*, ASCE (in press).
Seim, C. H., Herr, L., and Lin, T. Y. (1982). "Cable-stressed steel bridges." Paper presented to the TRB Committee on Steel Bridges, annual meeting, Transportation Research Board, Washington, D.C.
Stras, J. C. (1964). "An experimental and analytical study of prestressed composite beams," thesis presented to Rice University, Houston, Texas, in partial fulfillment of the requirements for the degree of Master of Science.
Tachibana, Y., Kondo, K., and Ito, K. (1964). "Experimental study on composite beams prestressed with wire cables." *Final report*, Intern. Assoc. for Bridge and Struct. Engrg., 7th Congress, Rio de Janeiro, 677–683.